Catalysis Science & Technology

ROYAL SOCIETY OF CHEMISTRY

PAPER

View Article Online
View Journal | View Issue

Cite this: *Catal. Sci. Technol.*, 2023, **13**, 187

Liquid-phase permethylation of diethylenetriamine using methanol over robust composite copper catalysts†

Fan Jiang,*[a] Zhen Yan,[a] Xuan Chen,[a] Xinlei Li,[a] Stéphane Streiff[a] and M. Pera-Titus *[ab]

Received 16th August 2022,
Accepted 20th November 2022

DOI: 10.1039/d2cy01454h

rsc.li/catalysis

Pentamethyldiethylenetriamine is a permethylated polyamine that is widely used to prepare foam polyurethane. The current technology for its synthesis relies on diethylenetriamine methylation with formaldehyde under H_2. This route is selective, but the use of formaldehyde raises safety and environmental concerns. Herein we present an alternative non-toxic route using methanol as greener and cheaper methylating reagent. The reaction proceeds fast and selectively over composite copper catalysts with a pentamethyldiethylenetriamine yield of 75% and resistance to sintering.

Introduction

The direct *N*-methylation of amines is a central chemical transformation for the synthesis of fine chemicals, pharmaceuticals and natural products.[1] Traditional *N*-methylation methods driven by direct nucleophilic substitution using methyl halides, dimethyl sulfate and diazomethane often suffer from low green footprint due to poor selectivity, use hazardous reactants and generation of salt waste.[2] *N*-Methylarylamines can also be prepared by Buchwald–Hartwig C–N coupling of methylamines with aryl halides in excess of base using palladium or nickel catalysts,[3] copper powder under air (Ullmann type),[4] or homogeneous copper in the presence of base (Buchwald–Taillefer).[5] These reactions can hardly be implemented to access aliphatic amines owing to the low stability and/or low reactivity of the alkylating metal intermediates.

Current industrial production of methylated amines relies on the reductive amination of formaldehyde (HCHO) with a hydrogen donor (*e.g.*, H_2). Formic acid (HCOOH) is also a C1 source for *N*-methylation in Eschweiler–Clarke methylation,[6] which can be conducted at room temperature with homogeneous ruthenium[7] or platinum (Karstedt) catalysts,[8] using hydrosilanes as reducing reagents. Recently, CO_2 was proposed as methylating agent using hydrosilanes,[9] hydroboranes,[10] borohydrides,[11] or H_2.[12] Dimethyl carbonate, prepared from CO_2 and methanol (MeOH), is an alternative *N*-methylation route.[13] As a rule, high temperatures (>150 °C) are required to promote methylation. Although a lower temperature (100 °C) protocol was developed for iron-[14] or nickel-based catalysts,[9d] excess hydrosilane is required as reducing agent.

To increase the green footprint and atom economy of *N*-methylation, it is highly desirable to develop efficient protocols using MeOH as green methylating reagent, where water is generated as main by-product.[15] To this aim, direct alcohol amination under the 'borrowing hydrogen' (BH_2) or 'hydrogen autotransfer' mechanism appears as an ideal approach, involving a net transfer of H_2 from the alcohol (*e.g.*, MeOH) to an intermediate imine or enamine.[16] Unlike reductive amination, no additional reductive species (usually H_2) is consumed for imine or enamine hydrogenation.

The earliest attempt to conduct direct amination reactions of fatty alkylamines with MeOH was reported in 1981 by Grigg *et al.* on *n*-butylamine using $RhH(PPh_3)_4$ (5 mol%) with 86% yield of the dimethylated amine at 100 °C for 96 h.[17] One year later, Arcelli *et al.* succeeded *N*-methylation of C_4-C_{12}-amines with $RuCl_2(PPh_3)_3$ (3 mol%) at 180 °C for 7 h. At large MeOH excess (15 eq), dimethylated amines were obtained with a yield up to 95%, while at lower excess (5 eq), monomethylated amines were favoured as main product.[18] Additional examples of ruthenium complexes were reported for *N*,*N*-dimethylation of alkylamines with MeOH at moderate temperature (40–100 °C) with good tolerance to reducible functional groups.[19] Also, Ir-type complexes were developed, but operating at higher temperature (>100 °C) and using a base (*e.g.*, Cs_2CO_3).[20]

[a] *Eco-Efficient Products and Processes Laboratory (E2P2L), UMI 3464 CNRS-Solvay, 3966 Jin Du Road, Xin Zhuang Ind. Zone, 201108 Shanghai, China. E-mail: fan.jiang@solvay.com*
[b] *Cardiff Catalysis Institute, School of Chemistry, Cardiff University, Main Building, Park Place, Cardiff CF10 3AT, UK. E-mail: peratitusm@cardiff.ac.uk*
† Electronic supplementary information (ESI) available. See DOI: https://doi.org/10.1039/d2cy01454h

Heterogeneous catalysts operating under the hydrogen borrowing mechanism have also been reported for *N*-methylation of alkylamines with MeOH. Alumina-supported CuO with acid–base additives (*e.g.*, ZnO) is known to catalyse the gas-phase *N*,*N*-dimethylation of C_1–C_4 amines after pre-reduction,[21] and *N*-methylation ethylenediamine at 200–250 °C.[22] In these examples, an external H_2 pressure is necessary to protect the copper phase against oxidation by the as-generated water in methanol during the reaction. Alumina-supported Ni and Pt nanoparticles can catalyse the gas-phase *N*,*N*-dimethylation of fatty amines using basic additives.[23] Tandem reactions were also reported over supported copper and chromium catalysts,[24] encompassing first the hydrogenation of dodecanonitrile in MeOH towards dodecylamine, followed by dimethylation to give *N*,*N*-dimethyldodecylamine at 250 °C and 50 bar H_2. Finally, examples of metal-supported photocatalysts have been documented for amine methylation at near-room temperature, comprising mainly aromatic and furfuryl amines (Au/TiO_2, Cu/TiO_2),[25] and to lesser extent aliphatic (Pd/TiO_2)[26] and cyclic amines (Ag/TiO_2),[27] with moderate-to-high yields.

Pentamethyldiethylenetriamine (PMDTA) is a permethylated polyamine that is employed industrially to prepare foam polyurethanes.[1b,28] The current technology for PMDTA synthesis relies on diethylenetriamine (DETA) methylation with an aqueous formaldehyde solution (37 wt%) as methyl source under H_2 (Scheme 1A).[29] This reaction is selective towards PMDTA, but the use of large excess of formaldehyde raises safety and environmental concerns. Herein we present an alternative route operating under the hydrogen borrowing mechanism for PMDTA synthesis from DETA using MeOH as a greener and cheaper methylating reagent (Scheme 1B). PMDTA formation proceeds first by dehydrogenation of MeOH to formaldehyde, followed by condensation of the latter with DETA to generate an imine/iminium salt intermediate, which is further hydrogenated to partially amine intermediates with ultimate formation of PMDTA. To this aim, a suitable hydrogen borrowing catalyst needs to be developed, which is the main purpose of this study.

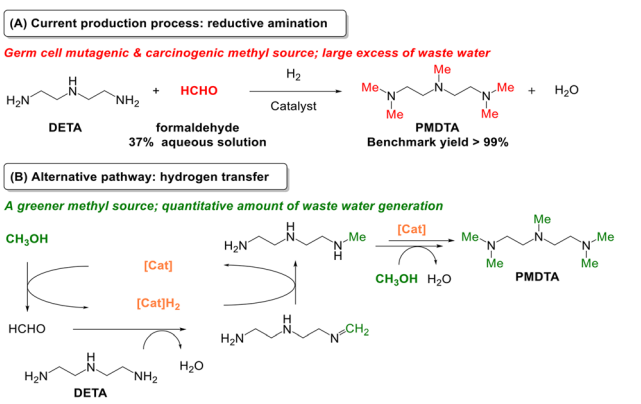

Scheme 1 (A) Current route for PMDTA synthesis from DETA and formaldehyde, and (B) alternative route for PMDTA synthesis from DETA and MeOH (CH_3OH) under the hydrogen borrowing mechanism.

Results and discussion

Catalyst screening

In our quest for an active and selective hydrogen borrowing catalyst to access PMDTA from DETA methylation with MeOH, we first screened benchmark (reductive) amination catalysts including RANEY® Ni, RANEY® Co and Ru/C,[30] as well as Pd/C. Since copper is known to favour secondary and tertiary amines by reaction of aliphatic alcohols with amines,[31] we also screened two copper catalysts including parent CuO (*i.e.* without binder, Cu_7), and composite CuO formulated with a binder (*e.g.*, silica, Cu_3) (see details in ESI,† Table S1). RANEY® Ni and RANEY® Co were tested without pre-reduction, whereas Ru/C, Pd/C, Cu_3 and Cu_7 were pre-reduced under H_2 (see ESI† for details).

The catalysts were screened at 200 °C for 18 h at low DETA concentration (1.0 wt% or MeOH/DETA (molar) = 371) under 30 bar H_2 pressure (Table 1). RANEY® Ni and RANEY® Co (entries 1–2) are both active for the reaction, but the PMDTA selectivity is low (7% and 23%, respectively). Ru/C is slightly less active with a DETA conversion of 88% and a very low PMDTA yield (3%) (entry 3). Likewise, the PMDTA yield is almost zero for Pd/C at full DETA conversion (entry 4). The composite Cu_3 catalyst displays the best performance with 54% PMDTA yield at full DETA conversion (entry 5). This result opposes the behaviour of Cu_7, with only 3.6% PMDTA yield at 63% DETA conversion (entry 6).

In all cases, the total selectivity does not reach 100% due to the formation of by-products. Representative chromatograms are depicted in Fig. 1. For instance, using Cu_3, cyclic (*i.e.* 1,4-dimethylpiperazine or DMP) and cleaved (tetramethylethylenediamine or TMEDA) appear as main by-products with retention times in the range 4.5–7.0 min (Fig. 1a, Scheme S1†). Analogous by-products are generated over RANEY® Co, together with partially methylated products (Fig. 1b) with retention times of 10–11 min. In the case, of Ru/C, different by-products are generated including partially methylated DETA, methyl-piperazine and aziridine derivatives, as inferred from GC–MS (Fig. 1c and S1†).

Table 1 Results of catalyst screening for DETA methylation[a]

Entry	Catalyst	DETA conversion/%	PMDTA yield/%
1	RANEY® Ni	100	7
2	RANEY® Co	100	23
3	Ru/C	88	3
4	Pd/C	100	0
5	Cu_3 – silica, nickel binder	100	54
6	Cu_7 – no binder	63	3.6

[a] Reaction conditions: 200 °C, 18 h, H_2 (30 bar), MeOH/DETA (molar) = 371, 260 mg of catalyst per 1 mmol of DETA.

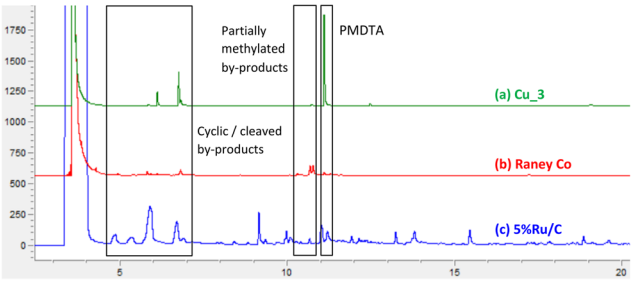

Fig. 1 Representative GC chromatogram of the reaction solution after DETA methylation over (a) Cu_3, (b) RANEY® Co and (c) 5%Ru/C catalysts. Reaction conditions: 200 °C, 18 h, H_2 (30 bar), MeOH/DETA (molar) = 371, 260 mg of catalyst per 1 mmol of DETA.

Additional by-products, issued from cleavage and polymerization, are also generated.

We further compared the performance of a series of composite Cu catalysts formulated with different binders (*e.g.*, silica, alumina, chromium oxide) (see composition in Table S1†). All the catalysts consist of CuO before pre-reduction, except Cu_5, showing also the presence of a minor amount of Cu_2O as inferred from XRD (not shown). All the catalysts exhibit a similar PMDTA selectivity (range 64–75%) at full DETA conversion (Fig. 2). Cu_1, Cu_2, Cu_5 and Cu_6, including silica (0.05–0.50 wt%) and/or chromium oxide (0.35–14 wt%) binders, display the highest DMP selectivity (range 11–15%). In contrast, the conversion decreases to less than 10% for Cu_3 and Cu_4 including a higher loading of silica binder (0.93 wt%) and an alumina binder (16 wt%), respectively. The TMEDA selectivity keeps low (<6%) for all catalysts. The missing selectivity to close the carbon balance is attributed to the formation of trimethylamine (TMA), which is detectable in the gas phase, and oligomers as inferred from GC analysis (Fig. S2†).

Overall, these results point out that, irrespective of the binder, all composite copper catalysts are selective for DETA methylation towards PMDTA. However, given its slightly lower DMP and TMEDA selectivity, Cu_3 was hereinafter used to optimize the catalytic performance as described in the following lines.

Catalytic performance of Cu_3

Effect of H_2 pressure. First, we explored the effect of the H_2 pressure on the catalytic performance of Cu_3. Either in the absence of H_2 or at low H_2 pressure (10 bar), the PMDTA selectivity is very low (3%) and partially methylated products are favoured (Fig. 3). In contrast, a H_2 pressure of 30 or 50 bar affords complete DETA methylation to PMDTA with a maximum yield of 77% at full DETA conversion. At 50 bar H_2, DMP and TMEDA are generated with the lowest selectivity, *i.e.* 8% and 2%, respectively.

The high H_2 pressure required to boost the reaction suggests that imine hydrogenation might be rate limiting for PMDTA synthesis compared to methanol dehydrogenation. Besides, H_2 is known to stabilize metal copper in amination reactions against nitride formation, coking and oxidation by as-generated water at the reaction conditions,[32] which can keep the copper phase active along the reaction.

Effect of reduction protocol. To survey the effect of the reduction protocol on the catalytic performance, Cu_3 was pre-reduced *ex situ* before reaction under a H_2/Ar = 1/10 atmosphere using a temperature ramp from 1 to 10 °C min^{-1}. Regardless of the temperature ramp, the samples are completely reduced according to the H_2-TPR profiles (Fig. S3†). However, the reduction peaks shift to higher temperature using higher temperature ramps.

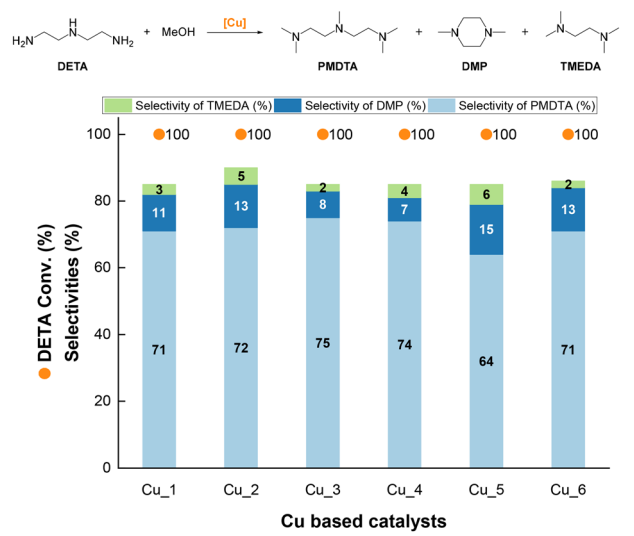

Fig. 2 Results of composite Cu catalyst screening for DETA methylation. Reaction conditions: 200 °C, 20 h, H_2 (50 bar), MeOH/DETA (molar) = 742, 140 mg of catalyst (64–109 mg Cu) per 1 mmol of DETA. The catalysts were pre-reduced from 50 °C to 200 °C using a temperature ramp of 1 °C min^{-1} before the reaction.

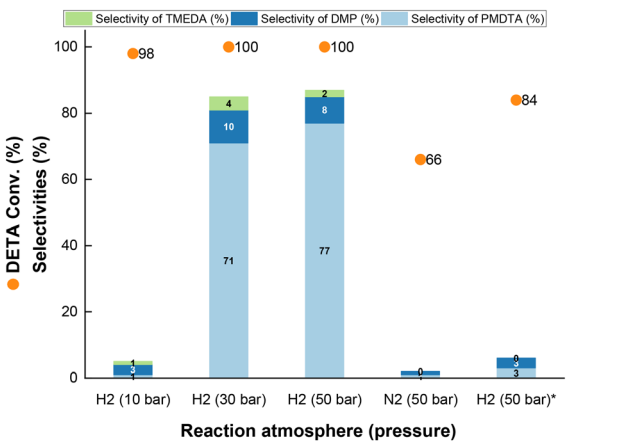

Fig. 3 Effect of H_2 pressure on the catalytic performance of Cu_3 for DETA methylation. Reaction conditions: 200 °C, 20 h, MeOH/DETA (molar) = 742, 90 mg of Cu_3 per 1 mmol of DETA. The catalyst was pre-reduced from 50 °C to 200 °C using a temperature ramp of 1 °C min^{-1} before the reaction. **In situ* catalyst reduction.

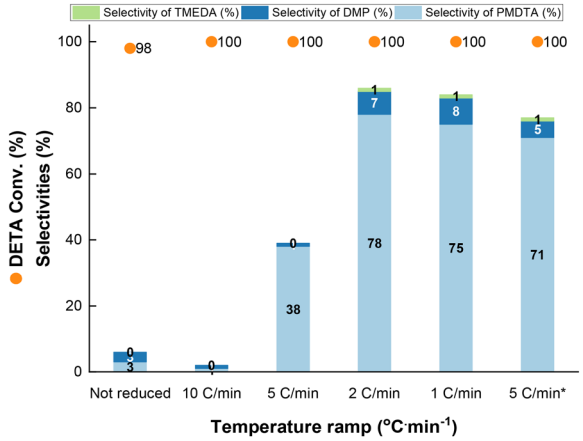

Fig. 4 Effect of the temperature ramp for Cu_3 pre-reduction on the catalytic performance for DETA methylation. Reaction conditions: 200 °C, 20 h, H_2 (50 bar), MeOH/DETA (molar) = 742, 140 mg of Cu_3 per 1 mmol of DETA, Cu_3 pre-reduction from 50 °C to 200 °C. *The maximum temperature for Cu_3 pre-reduction 185 °C instead of 200 °C.

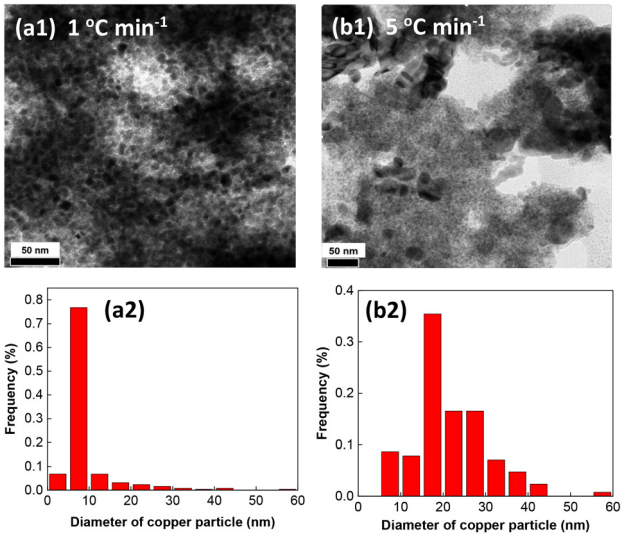

Fig. 5 Representative HR-TEM micrographs and size distribution of Cu_3 nanoparticles pre-reduced from 50 °C to 200 °C using a temperature ramp of (a1, a2) 1 °C min^{-1} and (b1, b2) 5 °C min^{-1}.

With these results in hand, the reaction was carried out at 200 °C and 50 bar H_2 pressure (Fig. 4). At lower ramps (*i.e.* 1 and 2 °C min^{-1}), the PMDTA selectivity is the highest (75–78%) with minor formation of DMP and TMEDA (8% and 1% selectivity, respectively), at full DETA conversion. Increasing the temperature ramp to 5 °C min^{-1}, the PMDTA selectivity decreases to 36% in favour of partially methylated products at full DETA conversion (Fig. S4†). Further increase of the ramp to 10 °C min^{-1} prevents PMDTA formation, whereas heavy products are generated, still at full DETA conversion. Interestingly, by keeping the temperature ramp at 5 °C min^{-1} but lowering the maximum temperature from 200 °C to 185 °C, the PMDTA selectivity increases to 71%.

The results above point out potential copper sintering during reduction at higher temperature ramps and reduction temperatures. Also, the temperature ramp might affect the final reduction state of copper.[32] To sort out between both effects, we conducted a comprehensive characterization study of Cu_3 by combining HR-TEM, XRD and XPS. HR-TEM clearly shows that the temperature ramp affects both the copper reducibility and morphology of the as-reduced particles. Using a temperature ramp of 1 °C min^{-1} results in copper particles with an average size of 9.2 nm (Fig. 5a1 and 2), while increasing the ramp to 5 and 10 °C min^{-1} results in larger sizes (>20 nm) (Fig. 5b1 and 2), which can be attributed to sintering. Sintering is even more obvious without binder (Fig. S5†), which explains the poor performance of Cu_7 (Table 1 entry 6).

The XRD patterns of Cu_3 show the presence of Cu^0 and Cu_2O phases after pre-reduction from 50 °C to 200 °C using temperature ramps of 1 °C min^{-1} and 5 °C min^{-1} (Fig. S6a–c1†). The deconvoluted XPS spectra of the Cu 2p core level of Cu_3 (Fig. S7a1 and 2†) shows bands with binding energies (BEs) centred at 932.4 eV (Cu $2p_{3/2}$) and 939.9 eV (Cu $2p_{1/2}$), and a complex set of satellite bands in the range 941.3–944.2 eV, that confirm the presence of Cu^0 and Cu_2O.[33] Besides, a band belonging to CuO is visible at a BE of 939.9 eV (Cu $2p_{3/2}$) and 943.1 eV (Cu $2p_{1/2}$), which can be attributed to partial passivation of the surface of copper particles upon exposure of the catalyst to ambient conditions. These bands are consistent with those observed for Cu_7 (without binder) (Fig. S8a†). The deconvoluted XPS spectra of the O1s core level (Fig. S7b1 and 2†) exhibit two bands with BEs at 530.6 eV and 531.2 eV that can be attributed to lattice oxygen $(O_L)^{2-}$ and oxygen defects/vacancies $(O_V)^{2-}$ in the copper oxide matrix, respectively.[33c] Two additional bands appear at 532.3 eV and 533.3 eV that are ascribed to Si–O–Si and Si–OH species, respectively.[34] The BE and intensity of the bands keep unchanged with the temperature ramp. The bands attributed to Cu–O and Cu–OH are also visible in the XPS spectra of Cu_7 (Fig. S8b†), but with lower intensity, which can be explained by a much higher particle sintering during pre-reduction compared to Cu_3.

Reaction mechanism

To gain insight into the reaction mechanism for PMDTA formation, we conducted additional catalytic tests at variable MeOH/DETA molar ratio and Cu_3 loading at optimized pre-reduction conditions. Keeping the MeOH/DETA molar ratio at 742, an increase of the catalyst loading from 30 to 90 mg of Cu_3 per 1 mmol of DETA promotes the PMDTA yield from 1% to 77% in detriment of partially methylated by-products, with concomitant increase of the DETA conversion from 90% to 100% (Fig. 6 and S9†). At 90 mg of Cu_3 per 1 mmol of DETA, a decrease of the MeOH/DETA molar ratio from 742 to 371 favours DMP formation instead of PMDTA. TMEDA is also generated as by-product, but the selectivity keeps almost unchanged with the MeOH/DETA ratio. The missing selectivity to 100% is attributed to partially methylated by-

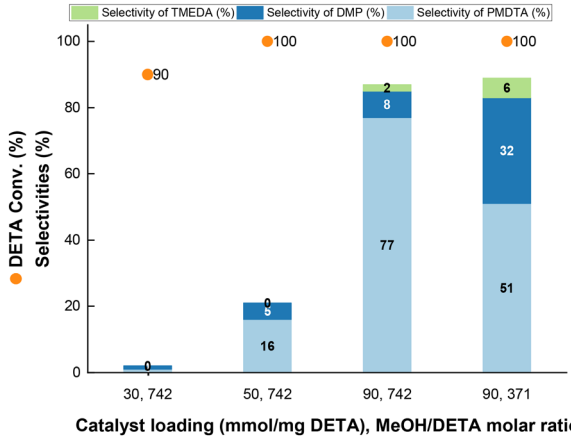

Fig. 6 Effect of MeOH/DETA molar ratio and Cu_3 loading on the catalytic performance for DETA methylation. Reaction conditions: 200 °C, 20 h, H_2 (50 bar), MeOH/DETA (molar) = 371 or 742, 30–90 mg of Cu_3 per 1 mmol of DETA. The catalyst was pre-reduced from 50 °C to 200 °C using a temperature ramp of 1 °C min^{-1} before the reaction.

products as inferred from GC analysis. Further increase of the MeOH/DETA molar ratio to 32 at 90 mg of Cu_3 per 1 mmol of DETA results in preferential DMP formation with 38% and 18% yield of DMP and PMDTA, respectively, at full DETA conversion.

To rationalize DMP formation from DETA cyclization, DETA was reacted over pre-reduced Cu_3 (Scheme 2). At neat conditions (*i.e.* without MeOH) (Scheme 2B), piperazine and TMEDA are formed with only 3% and 1% yield, respectively, at 27% DETA conversion, together with NH_3. In MeOH (Scheme 2A), DETA cyclization is expected to release *N*-methylamine ($MeNH_2$), which was otherwise not detected. This observation suggests that the methylated primary imine **2** is not a key intermediate for DMP formation. However, we cannot exclude that DMP is formed *via* this path from other di-, tri- or tetramethylated imine intermediates. These results point out that the primary imine from DETA (**1**) is an intermediate for piperazine formation, which could generate DMP by further methylation.

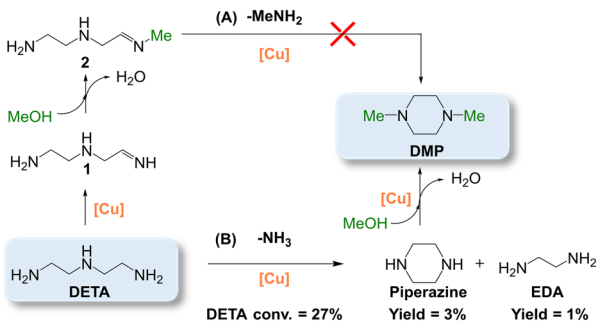

Scheme 2 Pathways to access DMP and TMEDA by reaction of DETA over Cu_3 with (A) and without (B) MeOH. Reaction conditions: 200 °C, 20 h, H_2 (50 bar), 187 mg of Cu_3 [Cu] per 1 mmol of DETA. The MeOH/DETA (molar) was 32 in (A). The catalyst was pre-reduced from 50 °C to 200 °C using a temperature ramp of 1 °C min^{-1} before the reaction.

Besides cyclization of intermediate **1** in Scheme 2A, DMP could be generated by transalkylation of PMDTA over Cu_3 according to the mechanism described by Wilson and Laine for transalkylation of tertiary amines (Scheme S2A and B†), also relying on the hydrogen borrowing mechanism.[35] First, one terminal tertiary amine group in PMDTA could dehydrogenate towards a quaternary imine intermediate with concomitant generation of a Cu–H species, followed by the formation of a Cu–iminium complex (species **II** in Scheme S2A†). Further nucleophilic attack by the other terminal amine group of the complex followed by cyclization and methyl transposition could generate a cyclic amine–iminium intermediate (species **IV** in Scheme S2A†) with simultaneous release of TMA. Finally, hydrogenation of the amine–iminium intermediate by Cu–H could generate DMP, and complete the catalytic cycle. Overall, this path would involve the transformation of 1 eq. of PMDTA into 1 eq. of DMP and 1 eq. of TMA (Scheme 3A).

In analogy, the middle tertiary amine group in PMDTA could also dehydrogenate towards a quaternary imine intermediate encompassing the formation of a Cu–iminium complex (species **II** in Scheme S2B†). Nucleophilic attack by the terminal tertiary amine of a second PMDTA molecule could generate a second Cu–iminium complex (species **IV** in Scheme S2B†) with concomitant release of one TMEDA molecule. Further nucleophilic attack by the other terminal amine group of the complex followed by cyclization and methyl transposition could generate the cyclic amine–iminium intermediate (species **VII** in Scheme S2B†) with simultaneous release of a second TMEDA molecule. Finally, hydrogenation of the amine–iminium intermediate by Cu–H could generate DMP, and complete the catalytic cycle. Overall, this path involves the transformation of 2 eq. of PMDTA into 1 eq. of DMP and 2 eq. of TMEDA (Scheme 3B).

To assess if the above mechanisms depicted in Scheme S2 and S3† are feasible in our catalytic system, we reacted PMDTA over Cu_3 at 200 °C for 20 h in MeOH (MeOH/DETA = 32 mol mol^{-1}). The DMP yield is 53% with TMA and TMEDA formation at 41% and 18% yield, respectively, and 72% DETA conversion. The combination of both mechanisms is consistent with the results obtained: the theoretical DMP yield is (TMA yield) +

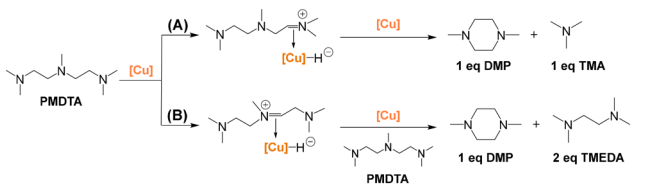

Scheme 3 Possible transalkylation paths for PMDTA transformation into DMP over Cu_3 [Cu] resulting in (A) TMA (1 eq. PMDTA) and (B) TMEDA (2 eq. PMDTA). Detailed catalytic cycles are provided in Scheme S2A and B.† Reaction conditions: 200 °C, 20 h, H_2 (50 bar), MeOH/PMDTA (molar) = 32, 100 mg of Cu_3 per 6 mmol of DETA. The catalyst was pre-reduced from 50 °C to 200 °C using a temperature ramp of 1 °C min^{-1} before the reaction.

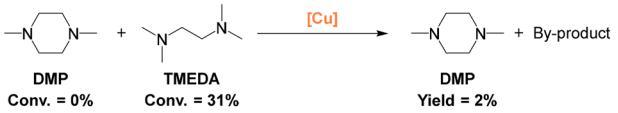

Scheme 4 DMP and TMEDA stability over Cu_3. Reaction conditions: 200 °C, 20 h, H_2 (50 bar), MeOH/PMDTA (molar) = 32, 100 mg of Cu_3 per 6 mmol of PMDTA. The catalyst was pre-reduced from 50 °C to 200 °C using a temperature ramp of 1 °C min^{-1} before the reaction.

(TMEDA yield)/2 = 41% + (18/2)% = 50%, which, within the limits of the experimental error and by assuming equal probability of occurrence, matches the experimental yield (53%). Overall, this observation points out that TMEDA is mainly generated from PMDTA transalkylation and that alternative pathways involving dehydrogenation and methanolysis are not favoured (Scheme S3†). Indeed, neither 2-methoxydimethylamine nor *N*,*N*-dimethyl-2-methoxyethylamine, which are expected by-products, was observed in our reaction system.

To further rationalize PMDTA transalkylation, DMP and TMEDA were reacted together in MeOH. The TMEDA conversion is 31%, while DMP is not converted and even shows a slight gain equivalent to 2% yield (Scheme 4). These results suggest very few yet detectable transformation of TMEDA into DMP, whereas most of the TMEDA converts into different by-products (not characterized), which is consistent with a higher thermodynamic stability of (cyclic) DMP compared to TMEDA. The high stability of DMP can be inferred from the high negative free energy of the transalkylation reaction in Scheme 3A (−53 kJ mol^{-1}), as computed by density functional theory (DFT) at the ωB97X-V/6-311+G (2DF,2P)//ωB97X-D/6-31G* level (gas phase calculation at 298 K, 1 bar) using Spartan v18.4.

Cu_3 recycling and reuse

The high activity and PMDTA selectivity over Cu_3 prompted us to study its recyclability and reuse. A dedicated study was carried out at 200 °C, 50 bar H_2 pressure using 90 mg of Cu_3 per 1 mmol of DETA by adding fresh DETA after each run. In all cases, full DETA conversion is reached, but the PMDTA selectivity decreases, especially after the 3rd run, in favour of DMP (Fig. 7). Also, traces of oligomers appear after the 3rd run (not shown). The average size of Cu particles evolves from 9.2 nm in the fresh catalyst (Fig. 5) to 13.5 nm after the 4th run (Fig. S10†), pointing out limited sintering. The catalyst keeps its integrity as inferred from the XRD patterns (Fig. S5†) and XPS spectra (Fig. S11†), with resistance to leaching.

Conclusions

Composite copper-based catalysts with different binders (*e.g.*, silica, chromium oxide) were found to work selectively for the synthesis of pentamethyldiethylenetriamine by permethylation of diethylenetriamine using methanol as methylating reagent. The maximum yield is 75%, and

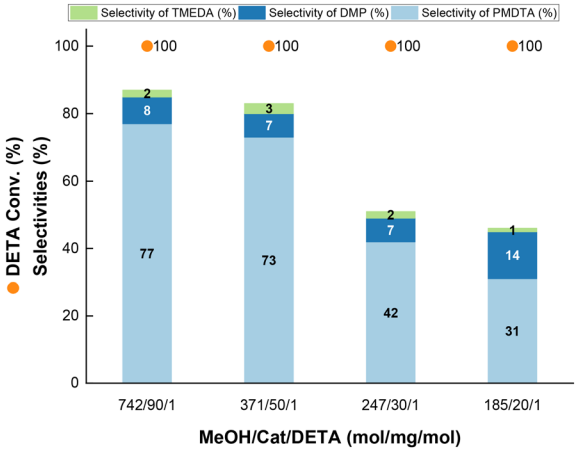

Fig. 7 Recyclability and reuse of Cu_3 for DETA methylation. Reaction conditions: 200 °C, 20 h, H_2 (50 bar), MeOH/DETA (molar) = 185–742, 20–90 mg of Cu_3 per 1 mmol of DETA. The catalyst was pre-reduced from 50 °C to 200 °C using a temperature ramp of 1 °C min^{-1} before the 1st run reaction.

copper–silica catalysts exhibit resistance to sintering and leaching at high DETA concentration and low catalyst loading. 1,4-Dimethylpiperazine is formed as main by-product driven most likely by catalytic cyclization of diethylenetriamine *via* a primary imine intermediate, followed by methylation, and/or transalkylation of pentamethyldiethylene triamine in methanol.

Author contributions

FJ: data curation, formal analysis, investigation, supervision, methodology, visualization, writing original draft, project administration; ZY: formal analysis, methodology, visualization, writing original draft; XC: investigation, formal analysis; XL: investigation, formal analysis; SS: conceptualization, funding acquisition, resources; MPT: conceptualization, funding acquisition, resources, supervision, validation, visualization, writing – review & editing.

Conflicts of interest

There are no conflicts to declare.

Acknowledgements

The authors are grateful to Solvay for funding. The authors also thank Dr Raphael Wischert from E2P2L for conducting thermodynamic calculations using Spartan and fruitful discussion on PMDTA transalkylation mechanisms.

References

1 (*a*) A. R. Cartolano and G. A. Vedage, *Kirk-Othmer, Encyclopedia of Chemical Technology*, John Wiley & Sons, Inc., NY, 2004, vol. 2, pp. 476–498; (*b*) S. A. Lawrence, *Amines: Synthesis, Properties and Applications*, Cambridge University

Press, 2004; (*c*) K. Natte, H. Neumann, M. Beller and R. V. Jagadeesh, *Angew. Chem., Int. Ed.*, 2017, **56**, 6384.
2 (*a*) R. N. Salvatore, C. H. Yoon and K. W. Jung, *Tetrahedron*, 2001, **57**, 7785; (*b*) G. Lamoureux and C. Agüero, *ARKIVOC*, 2009, **2009**, 251.
3 (*a*) R. J. Lundgren and M. Stradiotto, *Aldrichimica Acta*, 2012, **45**, 59; (*b*) C. Valente, S. Calimsiz, K. H. Hoi, D. Mallik, M. Sayah and M. G. Organ, *Angew. Chem., Int. Ed.*, 2012, **51**, 3314; (*c*) I. P. Beletskaya and A. V. Cheprakov, *Organometallics*, 2012, **31**, 7753.
4 J. Jiao, X.-R. Zhang, N.-H. Chang, J. Wang, J.-F. Wei, X.-Y. Shi and Z.-G. Chen, *J. Org. Chem.*, 2011, **76**, 1180.
5 (*a*) M. Taillefer, N. Xia and A. Ouali, *Angew. Chem., Int. Ed.*, 2007, **46**, 934; (*b*) H. Kaddouri, V. Vicente, A. Ouali, F. Ouazzani and M. Taillefer, *Angew. Chem., Int. Ed.*, 2009, **48**, 333; (*c*) G. Lefevre, G. Franc, A. Tlili, C. Adamo, M. Taillefer, I. Ciofini and A. Jutand, *Organometallics*, 2012, **31**, 7694.
6 (*a*) S. Kim, C. H. Oh, J. S. Ko, K. H. Ahn and Y. J. Kim, *J. Org. Chem.*, 1985, **50**, 1927; (*b*) S. Bhattacharyya, *Synth. Commun.*, 1995, **25**, 2061; (*c*) H. Alinezhad, M. Tajbakhsh and R. Zamani, *Synth. Commun.*, 2006, **36**, 3609.
7 S. Savourey, G. Lefevre, J.-C. Berthet and T. Cantat, *Chem. Commun.*, 2014, **50**, 14033.
8 I. Sorribes, K. Junge and M. Beller, *Chem. – Eur. J.*, 2014, **20**, 7878.
9 (*a*) Y. Li, X. Fang, K. Junge and M. Beller, *Angew. Chem., Int. Ed.*, 2013, **52**, 9568; (*b*) O. Jacquet, X. Frogneux, C. D. N. Gomes and T. Cantat, *Chem. Sci.*, 2013, **4**, 2127; (*c*) S. Das, F. D. Bobbink, G. Laurenczy and P. J. Dyson, *Angew. Chem., Int. Ed.*, 2014, **53**, 12876; (*d*) L. González-Sebastián, M. Flores-Alamo and J. J. García, *Organometallics*, 2015, **34**, 763; (*e*) H. Niu, L. Lu, R. Shi, C. Chiang and A. Lei, *Chem. Commun.*, 2017, **53**, 1148.
10 E. Blondiaux, J. Pouessel and T. Cantat, *Angew. Chem., Int. Ed.*, 2014, **53**, 12186.
11 Q. Zou, G. Long, T. Zhao and X. Hu, *Green Chem.*, 2020, **22**, 1134.
12 (*a*) Y. Li, I. Sorribes, T. Yan, K. Junge and M. Beller, *Angew. Chem., Int. Ed.*, 2013, **52**, 12156; (*b*) K. Beydoun, T. vom Stein, J. Klankermayer and W. Leitner, *Angew. Chem., Int. Ed.*, 2013, **52**, 9554; (*c*) A. Tlili, X. Frogneux, E. Blondiaux and T. Cantat, *Angew. Chem., Int. Ed.*, 2014, **53**, 2543; (*d*) X. Cui, Y. Zhang, Y. Deng and F. Shi, *Chem. Commun.*, 2014, **50**, 13521; (*e*) X. Cui, X. Dai, Y. Zhang, Y. Deng and F. Shi, *Chem. Sci.*, 2014, **5**, 649; (*f*) K. Beydoun, G. Ghattas, K. Thenert, J. Klankermayer and W. Leitner, *Angew. Chem., Int. Ed.*, 2014, **53**, 11010; (*g*) W. Lin, H. Cheng, Q. Wu, C. Zhang, M. Arai and F. Zhao, *ACS Catal.*, 2020, **10**, 3285.
13 (*a*) Z. L. Shen and X. Z. Jiang, *J. Mol. Catal. A: Chem.*, 2004, **213**, 193; (*b*) M. Selva, P. Tundo and T. Foccardi, *J. Org. Chem.*, 2005, **70**, 2476; (*c*) A. B. Shivarkar, S. P. Gupte and R. V. Chaudhari, *J. Mol. Catal. A: Chem.*, 2005, **226**, 49; (*d*) A. Dhakshinamoorthy, M. Alvaro and H. Garcia, *Appl. Catal., A*, 2010, **378**, 19; (*e*) X. L. Du, G. Tang, H. L. Bao, Z. Jiang, X. H. Zhong, D. S. Su and J. Q. Wang, *ChemSusChem*, 2015, **8**, 3489; (*f*) J. R. Cabrero-Antonino, R. Adam, J. Waerna, D. Y. Murzin and M. Beller, *Chem. Eng. J.*, 2018, **351**, 1129.
14 J. Zheng, C. Darcel and J.-B. Sortais, *Chem. Commun.*, 2014, **50**, 14229.
15 G. Yan, A. J. Borah, L. Wang and M. Yang, *Adv. Synth. Catal.*, 2015, **357**, 1333.
16 (*a*) G. Guillena, D. J. Ramon and M. Yus, *Chem. Rev.*, 2010, **110**, 1611; (*b*) G. E. Dobereiner and R. H. Crabtree, *Chem. Rev.*, 2010, **110**, 681; (*c*) C. Gunanathan and D. Milstein, *Science*, 2013, **341**, 1229712; (*d*) S. Bähn, S. Imm, L. Neubert, M. Zhang, H. Neumann and M. Beller, *ChemCatChem*, 2011, **3**, 1853.
17 R. Grigg, T. R. B. Mitchell, S. Sutthivaiyakit and N. Tongpenyai, *J. Chem. Soc., Chem. Commun.*, 1981, 611.
18 A. Arcelli, B.-T. Khai and G. Porzi, *J. Organomet. Chem.*, 1982, **235**, 93.
19 (*a*) G. Choi and S. H. Hong, *ACS Sustainable Chem. Eng.*, 2019, **7**, 524; (*b*) T. T. Dang, B. Ramalingam and A. M. Seayad, *ACS Catal.*, 2015, **5**, 4082.
20 R. Liang, S. Li, R. Wang, L. Lu and F. Li, *Org. Lett.*, 2017, **19**, 5790.
21 (*a*) S. Göbölös, M. Hegedüs, I. Kolosova, M. Maciejewski and J. L. Margitfalvi, *Appl. Catal., A*, 1988, **169**, 201; (*b*) Y. Pouilloux, V. Doidy, S. Hub, J. Kervennal and J. Barraul, *J. Mol. Catal. A: Chem.*, 1997, **115**, 317; (*c*) J. Simon, R. Becker, R. Lebkücher and H. Neuhauser, *US Pat.*, 5917039, 1999.
22 T. Yamakawa, I. Tsuchiya, D. Mitsuzuka and T. Ogawa, *Catal. Commun.*, 2004, **5**, 291.
23 (*a*) C. Forquy, *US Pat.*, 5254736, 1993; (*b*) Md. A. R. Jamil, A. S. Touchy, Md. N. Rashed, K. W. Ting, S. M. A. Siddiki, T. Toyao, Z. Maeno and K.-I. Shimizu, *J. Catal.*, 2019, **371**, 47.
24 J. Barrault, N. Essayem and C. Guimon, *Appl. Catal., A*, 1993, **102**, 151.
25 (*a*) L.-M. Wang, K. Jenkinson, A. E. H. Wheatley, K. Kuwata, S. Saito and H. Naka, *ACS Sustainable Chem. Eng.*, 2018, **6**, 15419; (*b*) L.-M. Wang, Y. Morioka, K. Jenkinson, A. E. H. Wheatley, S. Saito and H. Naka, *Sci. Rep.*, 2018, **8**, 6931; (*c*) B. Zhang, H. Gao and W. Wang, *Green Chem.*, 2020, **22**, 4433.
26 L. Zhang, Y. Zhang, Y. Deng and F. Shi, *RSC Adv.*, 2015, **5**, 14514.
27 V. N. Tsarev, Y. Morioka, J. Caner, Q. Wang, R. Ushimaru, A. Kudo, H. Naka and S. Saito, *Org. Lett.*, 2015, **17**, 2530.
28 *Amino Group Chemistry: From Synthesis to the Life Sciences*, ed. A. Ricci, Wiley-VCH: Weinheim, 2008.
29 M. Tanis and G. Rauniyar, *US Pat.*, 5105013, 1992.
30 (*a*) G. Rice, E. J. Kohn and L. W. Daasch, *J. Org. Chem.*, 1958, **23**, 1352; (*b*) K. Murugesan, V. G. Chandrashekhar, T. Senthamarai, R. V. Jagadeesh and M. Beller, *Nat. Protoc.*, 2020, **15**, 1313; (*c*) D. Ruiz, A. Aho, T. Saloranta, K. Eränen, J. Wärnå, R. Leino and D. Y. Murzin, *Chem. Eng. J.*, 2017, **307**, 739.
31 (*a*) A. Baiker and W. Richarz, *Ind. Eng. Chem. Prod. Res. Dev.*, 1977, **16**, 261; (*b*) R. C. Lemon, S. Depot and R. C. Myerly, *US Pat.*, 3022349, 1982; (*c*) A. Baiker, W. Caprez and W. L. Holstein, *Ind. Eng. Chem. Prod. Res. Dev.*, 1983, **22**, 217; (*d*)

M. Dixit, M. Mishra, P. A. Joshi and D. Shah, *Catal. Commun.*, 2013, **33**, 80; (*e*) F. Santoro, R. Psaro, N. Ravasio and F. Zaccheria, *ChemCatChem*, 2012, **4**, 1249.

32 (*a*) A. Baiker, *Ind. Eng. Chem. Prod. Res. Dev.*, 1981, **20**, 615; (*b*) F. Haese, A. Bottcher, B. Stein, W. Reif, J.-F. Melder, K.-H. Roβ, H. Rutter, S. Liang and S. Rittinger, *US Pat.*, 7405327B2, 2008.

33 (*a*) C. D. Wagner, W. M. Riggs, L. E. Davis and J. F. Mouler, *Handbook of X-Ray Photoelectron Spectroscopy*, ed. G. E. Muilenberg, Perkin Elmer Corporation, Physical Electronics Division, Eden Prairie, MN, 1979; (*b*) C. C. Chusuei, M. A. Brookshier and D. W. Goodman, *Langmuir*, 1999, **15**, 2806; (*c*) M. C. Biesinger, *Surf. Interface Anal.*, 2017, **49**, 1325.

34 (*a*) D. S. Jensen, S. S. Kanyal, N. Madaan, M. A. Vail, A. E. Dadson, M. H. Engelhard and M. R. Linford, *Surf. Sci. Spectra*, 2013, **20**, 36; (*b*) A. V. Naumkin, A. Kraut-Vass, S. W. Gaarenstroom and C. J. Powell, NIST X-ray Photoelectron Spectroscopy Database, Available online: **https://srdata.nist.gov/xps/** (accessed on 3rd October 2022).

35 R. B. Wilson Jr and R. M. Laine, *J. Am. Chem. Soc.*, 1985, **107**, 361.